doi: 10.1111/j.1472-8206.2007.00508.x

ORIGINAL ARTICLE

Empirical mode decomposition to assess cardiovascular autonomic control in rats

Edmundo Pereira de Souza Neto[a,b,c*], Patrice Abry[a], Patrick Loiseau[a], Jean Christophe Cejka[b], Marc Antoine Custaud[d], Jean Frutoso[b], Claude Gharib[b], Patrick Flandrin[a]

[a]*Laboratoire de Physique, CNRS UMR 5672, École Normale Supérieure de Lyon, 46, allée d'Italie, 69364 Lyon Cedex 07, France*

[b]*Université Claude Bernard Lyon I, Laboratoire de Physiologie, Faculté de Médecine Lyon Grange-Blanche, 8 avenue Rockefeller, 69373 Lyon Cedex 08, France*

[c]*Hospices Civils de Lyon, Groupement Hospitalier Est, Hôpital Neurologique Pierre Wertheimer, Service d'Anesthésie Réanimation, 59 boulevard Pinel, 69677, Bron Cedex, France*

[d]*Laboratoire de Physiologie d'Angers, UMR CNRS 6188, Faculté de médecine d'Angers, 49033 Angers Cedex, France*

Keywords
alpha gain,
autonomic nervous system,
blood pressure,
empirical mode decomposition,
LF/HF decomposition,
non-standard spectral analysis,
rats,
RR intervals

Received 25 July 2006;
revised 4 December 2006;
accepted 8 March 2007

*Correspondence and reprints:
edmundo.pereira-de-souza-neto@chu-lyon.fr

ABSTRACT

Heart beat rate and blood pressure, together with baroreflex sensitivity, have become important tools in assessing cardiac autonomic system control and in studying sympathovagal balance. These analyses are usually performed thanks to spectral indices computed from standard spectral analysis techniques. However, standard spectral analysis and its corresponding rigid band-pass filter formulation suffer from two major drawbacks. It can be significantly distorted by non-stationarity issues and it proves unable to adjust to natural intra- and inter-individual variability. Empirical mode decomposition (EMD), a tool recently introduced in the literature, provides us with a signal-adaptive decomposition that proves useful for the analysis of non-stationary data and shows a strong capability to precisely adjust to the spectral content of the analyzed data. It is based on the concept that any complicated set of data can be decomposed into a finite number of components, called intrinsic mode functions, associated with different spectral contributions. The aims of this study were twofold. First, we studied the changes in the sympathovagal balance induced by various pharmacological blockades (phentolamine, atropine and atenolol) of the autonomic nervous system in normotensive rats. Secondly, we assessed the use of EMD for the analysis of the cardiac sympathovagal balance after pharmacological injections. For this, we developed a new (EMD-based) low frequency vs. high frequency spectral decomposition of heart beat variability and systolic blood pressure, we define the corresponding EMD spectral indices and study their relevance to detect and analyze changes accurately in the sympathovagal balance without having recourse to any a priori fixed high-pass/low-pass filters.

MOTIVATION AND POSITION OF THE PROBLEM

Complex interactions exist between the sympathetic and parasympathetic systems, the two components of the autonomic nervous system, which act as a balance between competing neural mechanisms. Under selected stimulations, the dynamics of this balance mechanisms can be significantly altered [1]. Such modifications can be studied using relevant autonomic indices [2].

'Heart rate variability (HRV)' is a general term used to denote fluctuations in inter-beat intervals (i.e.

intervals between consecutive heart beats or RR intervals) and therefore in instantaneous heart rate. The analysis of heart rate variability has become increasingly important in physiological studies and the support for using heart rate variability as an index for autonomic cardiovascular control comes from results demonstrating that heart rate variability is virtually abolished after parasympathetic and sympathetic blockades [3–5].

Heart rate variability indices [such as the ratio between the powers of the low and high frequencies, or the normalized low-frequency (LF) and high-frequency (HF) powers] have been used to describe the sympathovagal balance [1,5,6]. Under normal circumstances, HF power represents the vagal control of the heart, modulated by breathing, while LF power (more precisely, its normalized version) reflects primarily the sympathetic modulation of heart rate [6]. Finally, the LF/HF ratio characterizes the sympathovagal balance [5,6]. However, other studies also suggest that LF heart rate rhythms may have both sympathetic and vagal origins [7,8].

Although blood pressure is continuously modified by external stimulations, it spontaneously tends to return to a stable point. When blood pressure decreases or rises, the baroreceptor activity influences heart rate and myocardial contractility, in order to adapt cardiac output. Thus, baroreflex is important to counteract depressor or pressor stimuli and to cause arterial pressure to return to normal levels [9].

Quantitative analyses of the overall gains of baroreflex are commonly performed in terms of ratios of powers of the frequency contents of the RR intervals and systolic blood pressure (SBP) variations. Hence, spectral analysis has become a standard to study baroreflex and periodogram-based estimates, or autoregressive models are commonly used for the analysis of the corresponding data [3,6,10]. Such methods, which in most cases generate comparable results, fundamentally rely on the assumption that the data are stationary and linear in nature. However, there are situations where these assumptions are no longer valid. For instance, a sudden change can be imposed over the studied system or patient [11]. Moreover, the spectral content of the data under study may spontaneously vary because it is naturally tied to a time-varying phenomenon (such as respiration). Moreover, baroreflex index definitions rely on the choice of an a priori and rigid LF–HF decomposition. Such an approach cannot account for the unavoidable intra- or inter-individual variability that naturally occurs. Therefore, to cope both with non-stationarity and natural variability issues, we propose to use a non-standard spectral analysis based on a new approach, referred to as empirical mode decomposition (EMD) [12,13].

The aims of the present study were twofold. First, we intended to assess the use of the EMD to perform (non-standard) spectral analysis so as to adaptively separate HF and LF components of RR intervals and SBP, and hence to analyze baroreflex sensitivity. Secondly, we proposed to compare the relevance and benefits of the use of EMD-based autonomic indices vs. standard indices for the characterization of cardiac sympathovagal balance. This was achieved by performing adrenergic and cholinergic receptor blockades in a population of normotensive rats. Changes in the corresponding indices were studied after the pharmacological blockade of the autonomic nervous system.

MATERIALS AND METHODS

Animals

After a 10-day quarantine period, eight male Wistar rats (body weight 270 ± 20 g; IFFA-CREDO™, Les Oncins, France) were used. They were housed in controlled conditions of temperature (22 ± 1 °C), humidity (60 ± 10%), and lighting [12-h light/dark cycle, 7:00 AM to 7:00 PM (light) and 7:00 PM to 7:00 AM (dark)]. They were fed standard rat chow containing 0.3% sodium (Elevage UAR, Epinay sur Orge, France) and tap water ad libitum. The protocol was in accordance with the *Guide for the Care and Use of Laboratory Animals* published by the US National Institutes of Health (NIH Publication No. 85-23, revised 1996).

Telemetry system

The telemetry system was purchased from Data Sciences International™ (St Paul, MN, USA). It is composed of an implantable transmitter Tl 11-M2-C50-PXT, a receiver RLA 1020, a pressure reference module C11 PR, a data acquisition system with a consolidation matrix BCM 100, for converting the radio-signal to electrical impulses, and a computer with a UA10 PC processor card for data recording and storing.

Surgical implantation

The rats were anesthetized with halothane (2% in oxygen). The telemetry transmitter was implanted 14 days before the study under aseptic conditions into

the peritoneal cavity with the sensing catheter placed in the descending aorta below the renal arteries. Transmitter leads were sutured subcutaneously to the dorsal surface of the xiphoid process and into the anterior mediastinum close to the right atrium.

Body temperature was maintained at 38 °C using an electric heating pad during and after surgery until rats awakened. During the post-surgical period, the animals were administered penicillin (15 000 units s.c.) and buprenorphine (0.03 mg/kg s.c.) for 3 days and monitored for general health and blood pressure, pulse, and heart rate. Subsequently, 3 days before the study, rats were re-anesthetized with halothane (2%in oxygen), and a polyethylene catheter (no. 2, inner diameter 0.38 mm, outer diameter 1.09 mm; Biotrol™, Paris, France) was inserted into the lower inferior cava vein via the left femoral vein. The catheter was filled with heparinized saline (50 U heparin/mL) and plugged with a short piece of stainless steel wire.

Experimental protocol

Four types of injections were performed:

- Saline 0.9% (100 μg/kg i.v.; $n = 8$);
- Phentolamine (5 mg/kg i.v., 10 mg/mL, Sigma Chemical, St Louis, MO, USA; $n = 8$);
- Atropine (0.5 mg/kg i.v., 10 mg/mL, Sigma; $n = 8$);
- Atenolol (1 mg/kg i.v., 10 mg/mL, Sigma; $n = 8$).

RR intervals and SBP reflect the changes in the sympathovagal balance state induced by pharmacological blockades of the autonomic nervous system: a decrease of the parasympathetic effect after atropine administration or a decrease of the sympathetic effect after atenolol administration.

The rats were kept individually in a plexiglass cages placed above the receiver. Each rat was subjected to a total of four treatments, with one injection per day (performed individually every other day). The order of treatments was randomized for each rat, and hence a cumulative effect was improbable. Agonists were injected at the end of the recording to confirm adequate blockade. β1-adrenergic blockade was demonstrated by the suppression of tachycardia after isoproterenol administration (0.2 μg/kg i.v., Sigma). The efficacy of α1-blockade by phentolamine was assessed by the measurement of pressor responses to an intravenous injection of the alpha-adrenoceptor agonist phenylephrine (3 μg/kg i.v., Sigma). Blood pressure and heart rate responses to metacholine (0.1 μg/kg i.v., Sigma) were used to insure the efficacy of the cholinergic receptor blockade.

Data recording

RR intervals and arterial blood pressure were monitored before and after the injections. Data recording was performed only if the rats showed no sign of infection and had normal weight gain. Recording sessions were always performed between 9:00 AM and 12:00 AM, over a period of 15 min for each injection. Continuous data acquisition (ECG and blood pressure) at a sampling rate of 1000 Hz, was done on a PC (Pentium™ 133 MHz with a 12-bit analogue-to-digital converter, AT-MIO-16E-10; National Instruments™, Austin, TX, USA), equipped with a software developed with LabVIEW 4.0.1 software™ (National Instruments™, Austin, TX, USA).

For each cardiac cycle, heart beat occurrence times, $\{t_i\}$, were extracted (from the ECG signal) and the systolic and diastolic blood pressures were recorded at the corresponding times. Premature and post-extrasystolic beats were manually identified and edited by linear interpolation. Such beats represented <2% of all analyzed beats. The data analyzed in the present study therefore consist of the list of the RR intervals, $\{R_i = t_{i+1} - t_i, i \in I\}$, together with the corresponding SBP, $\{P_i = \mathrm{SBP}(t_i), i \in I\}$ and are hence irregularly sampled.

DATA ANALYSIS

Preprocessing

To transform the recorded data into a regularly sampled time series, the following preprocessing procedures were applied.

1. A sliding median filter was first applied to the RR intervals and SBP series to replace outliers and/or abnormal values with a local average.
2. RR intervals and SBP series were independently and regularly resampled with sampling frequency: $f_e = 10$ Hz. It was chosen high a priori with respect to the naturally expected frequency content of the data. It was checked a posteriori that Shannon criterion was well satisfied.
3. A standard linear detrending procedure was systematically applied independently on both time series.
4. Because they present significant, very low-frequency (VLF) components related to various phenomena (such as respiration) that are not of interest for the present study, the data were high-pass filtered. Based on results recalled below, the cut-off frequency is: $f_c = 0.25$ Hz. This last operation was omitted when data were analyzed with EMD.

In the sequel, the data obtained from these operations will be denoted, with a little abuse of notation, $\{R_k = R(kT_e), k \in N\}$ and $\{P_k = P(kT_e), k \in N\}$, where $T_e = 1/f_e$ and N denotes the set of positive integers. Examples of such time series are shown in *Figures 1* and *2*, top rows.

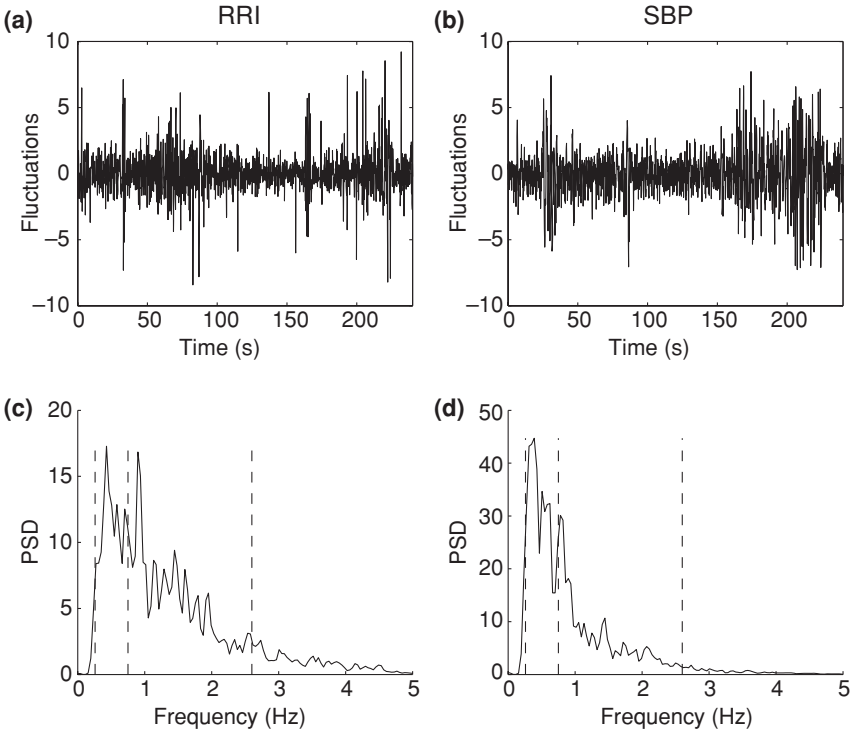

Figure 1 Example 1. For a chosen rat (phentolamine injection): left column, RR Intervals (RRI, in ms); right column, systolic blood pressure (SBP, in mmHg); top row, time series; bottom row, power spectral densities estimates (in 10^3ms^2/Hz for RRI and 10^3mmHg^2/Hz for SBP), obtained from periodograms. The vertical dashed lines indicate the VLF, LF and HF rigid a priori frequency bands. Equivalent plots for each rat and each injection are available upon request. HF = high frequency; LF = low frequency; VLF = very low frequency.

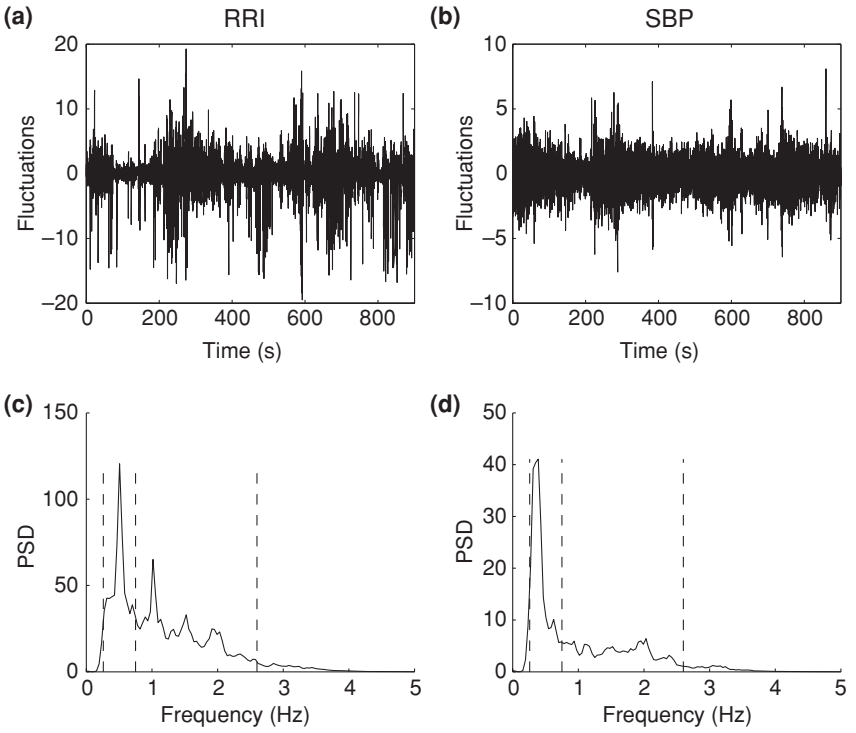

Figure 2 Example 2. For a chosen rat (no injection): left column, RR Intervals (RRI, in ms); right column, systolic blood pressure (SBP, in mmHg); top row, time series; bottom row, power spectral densities estimates (in 10^3ms^2/Hz for RRI and 10^3mmHg^2/Hz for SBP) obtained from periodograms. The vertical dashed lines indicate the VLF, LF and HF rigid a priori frequency bands. Equivalent plots for each rat and each injection are available upon request. HF = high frequency; LF = low frequency; VLF = very low frequency.

Standard spectral analysis and baroreflex sensitivity

LH vs. HF decomposition

The spectra, or power spectral densities (PSD), of the time series, as well as the cross spectrum, were computed using a standard periodogram spectral estimator (Hamming window). Estimated spectra were labeled S_R, S_P and S_{RP}, respectively. Examples are reported in *Figures 1* and *2*, bottom rows.

Spectra are usually divided into three frequency bands appropriate to the cardiac frequency of the rat [14]:

- Very low frequency (VLF): $f_{VLF,L} = 0.0195 \leq f \leq f_{VLF,H} = 0.26$ Hz;
- Low frequency (LF): $f_{LF,L} = 0.26 \leq f \leq f_{LF,H} = 0.75$ Hz;
- High frequency (HF): $f_{HF,L} = 0.75 \leq f \leq f_{HF,H} = 4.00$ Hz.

The VLF oscillations are not studied. Absolute powers of each frequency band are computed by integrating PSD across the a priori chosen frequency bands:

$$P_{R,LF} = \int_{f_{LF,L}}^{f_{LF,H}} S_R(f)\mathrm{d}f, \quad P_{R,HF} = \int_{f_{HF,L}}^{f_{HF,F}} S_R(f)\mathrm{d}f,$$
$$P_{P,LF} = \int_{f_{LF,L}}^{f_{LF,H}} S_P(f)\mathrm{d}f, \quad P_{P,HF} = \int_{f_{HF,L}}^{f_{HF,F}} S_P(f)\mathrm{d}f. \tag{1}$$

The ratio LF/HF is defined as:

$$\frac{LF}{HF} = \frac{P_{R,LF}}{P_{R,HF}} \tag{2}$$

Normalized powers enable us to perform comparisons between animals that are characterized by large variations in absolute PSDs. They are obtained by dividing the integrated PSDs within each frequency band (LF or HF) by the sum of the LF and HF absolute PSDs:

$$\tilde{P}_{R,LF} = \frac{P_{R,LF}}{P_{R,LF} + P_{R,HF}},$$
$$\tilde{P}_{R,HF} = \frac{P_{R,HF}}{P_{R,LF} + P_{R,HF}},$$
$$\tilde{P}_{P,LF} = \frac{P_{P,LF}}{P_{P,LF} + P_{P,HF}},$$
$$\tilde{P}_{P,HF} = \frac{P_{P,HF}}{P_{P,LF} + P_{P,HF}}. \tag{3}$$

Baroreflex sensitivity and alpha gains

The barosensitivity consists of the regulation mechanism that interrelates the fluctuations of RR intervals to that of SBP. It can be characterized via two numbers referred to as the LF and HF alpha gains, which are defined as:

$$\alpha_{LF} = \int_{f_{LF,L}}^{f_{LF,H}} \gamma(f)\sqrt{\frac{S_R(f)}{S_P(f)}}\mathrm{d}f, \quad \alpha_{HF} = \int_{f_{HF,L}}^{f_{HF,H}} \gamma(f)\sqrt{\frac{S_R(f)}{S_P(f)}}\mathrm{d}f, \tag{4}$$

where the coherence function γ is defined as:

$$\gamma(f) = \frac{S_{RP}(f)}{\sqrt{S_R(f)S_P(f)}}. \tag{5}$$

EMD and baroreflex sensitivity

In a recent study, we proposed to define extensions of these alpha gains that allowed us to study the evolution along time of the barosensitivity and derived the corresponding algorithm [15]. However, in this study, we mostly wanted to be able to account for natural intra- and inter-individual variabilities. For this, we proposed the use of a non-standard spectral analysis based on the EMD.

EMD

The starting point of EMD is to consider oscillations at a very local level. In fact, when looking at the evolution of a signal $X(t)$ between two consecutive extrema (say, two minima $m-$ and $m+$, occurring at times $t-$ and $t+$ respectively), it becomes possible to heuristically define a (local) high-frequency part $d(t)$, or local detail, which corresponds to the oscillation terminating at the two minima and passing through the maximum M, that necessarily exists in between $m-$ and $m+$. For the picture to be complete, one still has to identify the corresponding (local) low-frequency part $m(t)$, or local trend, so that we have $X(t) = m(t) + d(t)$ for $t- < t < t+$. Assuming this is done in some proper way for all the oscillations composing the entire signal, the procedure can then be applied on the residual consisting of all local trends. Constitutive components of a signal can therefore be iteratively extracted this way, the only definition of such a so-extracted 'component', referred to as an intrinsic mode function (IMF), which is locally (i.e. at the scale of a single oscillation) in the highest frequency band. Given a signal $X(t)$, the effective algorithm of EMD is as follows:

1. identify all extrema of $X(t)$;
2. interpolate between minima (resp. maxima), ending up with some 'envelope' $e_n(t)$ [resp. $e_M(t)$];
3. compute the average $m(t) = \{e_n(t) + e_m(t)\}/2$;
4. extract the first 'mode' as $d(t) = X(t) - m(t)$;
5. iterate on the residual $m(t)$.

In practice, the above procedure has to be refined by first iterating steps 1 to 4 upon the detail signal $d(t)$, until this can be considered as a zero mean according to some

stopping criterion – this is usually referred to as the sifting procedure [12]. The aims of this repeated operation are to eliminate the riding waves and to achieve a more symmetrical wave profile by smoothing the uneven amplitudes. It is suggested that a threshold is used, computed by summing the squared normalized differences from two consecutive sifting results, between 0.2 and 0.4 as a limit, to obtain the desired IMF-first component [12,16–18]. Once this is achieved, the detail is considered as the effective IMF, the corresponding residual is computed and step 5 applies.

An IMF satisfies two conditions: in the whole dataset, the number of extrema and the number of zero crossings must either equal or differ at most by 1; and at any point, the mean value of the envelope defined by the local maxima and the envelope defined by the local minima is 0 [17]. By construction, the number of extrema is decreased (on average, by a factor of 2) when going from one residual to the next. Modes and residuals are determined on spectral arguments, but it is worth stressing the fact that their HF vs. LF discrimination applies only locally and corresponds by no way to a predetermined sub-band filtering (as, e.g. in a wavelet transform). Selection of modes rather corresponds to an automatic and adaptive and hence signal-dependent (and possibly time-variant) filtering.

Given an input signal X to be analyzed, the output of the EMD procedure therefore consists of a set of IMFs whose number and contents are both signal- and procedure parameter-dependent. IMFs are numbered in increasing order $IMF_{X,1}$, $IMF_{X,2}$,… from HF to LF contents.

IMF association

Because IMFs are adaptively or self-chosen by the data under analysis, there is no reason why they should naturally match the rigid a priori VLF, LF and HF bandwidth division mentioned above. To be able to perform an EMD-based analysis of the baroreflex sensitivity, we need to re-define EMD-based LF and HF components. Based on observations detailed and made explicit in the section '*IMF Frequency Contents and EMD-based LF and HF Decomposition*', we are able to define the HF and LF contributions of the RR intervals and SBP time series by addition of well-chosen IMFs (precise definitions are relegated to the above-mentioned section). They are labeled, R_{LF}, R_{HF}, P_{LF}, P_{HF} and $S_{R,LF}$, $S_{R,HF}$, $S_{P,LF}$ and $S_{P,HF}$ stand for their power spectra, respectively. From those LF and HF components, the corresponding spectral indices can be defined (the 'prime' symbols are added to distinguish the EMD-based quantities from the standard ones):

$$
\begin{aligned}
&P'_{R,LF} = \int S_{R,LF}(f)\mathrm{d}f, \quad P'_{R,HF} = \int S_{R,HF}(f)\mathrm{d}f,\\
&P'_{P,LF} = \int S_{P,LF}(f)\mathrm{d}f, \quad P'_{P,HF} = \int S_{P,HF}(f)\mathrm{d}f,\\
&\left(\frac{LF}{HF}\right)' = \frac{P'_{R,LF}}{P'_{R,HF}}\\
&\tilde{P}'_{R,LF} = \frac{P'_{R,LF}}{P'_{R,LF} + P'_{R,HF}} \quad \tilde{P}'_{R,HF} = \frac{P'_{R,HF}}{P'_{R,LF} + P'_{R,HF}}\\
&\tilde{P}'_{P,LF} = \frac{P'_{P,LF}}{P'_{P,LF} + P'_{P,HF}} \quad \tilde{P}'_{P,HF} = \frac{P'_{P,HF}}{P'_{P,LF} + P'_{P,HF}}.
\end{aligned}
\tag{6}
$$

Baroreflex sensitivity: EMD-based alpha gains

Because we no longer have two time series, R and P, but four, R_{HF}, R_{LF}, P_{HF} and P_{LF} to characterize baroreflex sensitivity, we can no longer apply the alpha gains as defined in Eqn (4) above. We propose the following EMD extensions of these indices.

$$
\begin{aligned}
\alpha'_{LF} &= \int_{\bar{f}_{P,LF}-\beta\Delta f_{P,LF}}^{\bar{f}_{P,LF}+\beta\Delta f_{P,LF}} \gamma_{LF}(f)\sqrt{\frac{S_{R,LF}(f)}{S_{P,LF}(f)}}\mathrm{d}f,\\
\alpha'_{HF} &= \int_{\bar{f}_{P,HF}-\beta\Delta f_{P,HF}}^{\bar{f}_{P,HF}+\beta\Delta f_{P,HF}} \gamma_{HF}(f)\sqrt{\frac{S_{R,HF}(f)}{S_{P,HF}(f)}}\mathrm{d}f,
\end{aligned}
\tag{7}
$$

The central frequencies, $\bar{f}_{P,LF}$, $\bar{f}_{P,HF}$, the standard deviation spectral extensions, $f\Delta f_{P,LF}$, $\Delta f_{P,HF}$, and the coherence functions, γ'_{LF}, γ'_{HF}, are defined as:

$$
\begin{aligned}
\bar{f}_{P,LF} &= \frac{\int f.S_{P,LF}(f)\mathrm{d}f}{\int S_{P,LF}(f)\mathrm{d}f,}\\
\Delta f_{P,LF} &= \left(\frac{\int (f-\bar{f}_{P,LF})^2 S_{P,LF}(f)\mathrm{d}f}{\int S_{P,LF}(f)\mathrm{d}f}\right)^{1/2},\\
\gamma'_{LF}(f) &= \frac{S_{RP,LF}(f)}{\sqrt{S_{R,LF}(f)S_{P,LF}(f)}}.
\end{aligned}
\tag{8}
$$

For HF quantities, the corresponding definitions hold changing LH into HF.

The definition of α'_{LF} (resp., of α'_{HF}) involves a division by P_{LF} (resp., P_{HF}). By construction, P_{LF} (resp., P_{HF}) is a band-pass process and it is experimentally observed that its spectrum mostly vanishes $\bar{f}_{P,LF} - 2\Delta f_{P,LF} \leq f \leq \bar{f}_{P,LF} + 2\Delta f_{P,LF}$ (resp., $\bar{f}_{P,HF} - 2\Delta f_{P,HF} \leq f \leq \bar{f}_{P,HF} + 2\Delta f_{P,HF}$) (cf. *Figures 7* and *8*). This leads us to restrict accordingly the integration range, making use of the tunable parameter $\beta > 0$ whose precise choice will be further discussed (cf. Section *EMD Alpha Gains: Choosing the β Parameter*). Obviously, R_{HF} and R_{LF} also consist of

band-pass processes. Because they are involved in the numerator of the EMD gain definitions, they do not imply any restriction. Moreover, for most cases, it can be observed that $f_{P,LF}$, $\Delta f_{P,LF}$ and $f_{R,LF}$, $\Delta f_{R,LF}$ closely coincide (resp., $f_{P,HF}$, $\Delta f_{P,HF}$ and $f_{R,HF}$, $\Delta f_{R,HF}$).

Statistical tests and significant changes

Non-parametric Friedman's test associated with the Wilcoxon matched-pairs test, corrected for multiple comparisons, was performed for comparisons between base, saline, α1- , β1- and cholinergic blockades. Wilcoxon's test for paired data was used to study agonist effects before and after blockade. Statistical analysis was performed using the StatView™ software for Windows (1996, version 4.57; Abacus Concepts Inc., Berkeley, CA, USA). Results are reported in tables (cf. *Tables I–IV*) and are expressed in terms of median ± median absolute deviation. The usual $P \leq 5\%$ significance level is used and significant changes are marked with asterisks in tables.

Analysis routines

The EMD procedures and the corresponding non-standard spectral analysis as well as the standard one and the change test were developed by our team in Matlab, Mathworks™ (Natick, MA, USA), using the signal processing and statistical toolboxes, together with the Time-Frequency toolbox [19]. The EMD codes are available at perso.ens-lyon.fr/patrick.flandrin.

EMD PROCEDURE: PRACTICAL ISSUES, HF/LF DECOMPOSITION AND ALPHA GAINS

Prior to describing the results obtained on the sympatovagal balance analysis (cf. section *Experimental Results*),

Table I Time domain measures of RR intervals, systolic and diastolic blood pressures in different experimental conditions.

	Control	Saline (0.9%)	Phentolamine (10 mg/mL)	Atropine (10 mg/mL)	Atenolol (10 mg/mL)
RR intervals (ms)	170 ± 3	172 ± 5	122 ± 4*	128 ± 5*	188 ± 3*
SBP (mmHg)	121 ± 5	125 ± 7	95 ± 7*	135 ± 6*	110 ± 8*
DBP (mmHg)	92 ± 3	90 ± 5	76 ± 3*	107 ± 2*	80 ± 3*

Time-domain measures of RR intervals, systolic (SBP) and diastolic (DBP) blood pressures in different experimental conditions for eight conscious rats.
Results are expressed in terms of median ± median absolute deviation and values with '*' indicate a significant change compared with the control value (as detected using a non-parametric Friedman test, cf. section *Statistical Tests and Significant Changes*).

Table II Standard vs. EMD-based spectral analysis indices for RR intervals.

	Control	Saline (0.9%)	Phentolamine (10 mg/mL)	Atropine (10 mg/mL)	Atenolol (10 mg/mL)
Standard					
$P_{R,LF}$	0.36 ± 0.16	0.43 ± 0.23	0.14 ± 0.67	0.15 ± 0.13*	0.43 ± 0.43
$P_{R,HF}$	0.56 ± 0.22	0.62 ± 0.24	0.26 ± 0.94	0.10 ± 0.10*	0.92 ± 1.10
$\tilde{P}_{R,LF}$	0.41 ± 0.03	0.40 ± 0.04	0.37 ± 0.07	0.52 ± 0.10*	0.31 ± 0.10
$\tilde{P}_{R,HF}$	0.59 ± 0.03	0.60 ± 0.04	0.63 ± 0.07	0.48 ± 0.10*	0.69 ± 0.10
LF/HF	0.68 ± 0.08	0.67 ± 0.12	0.58 ± 0.17	1.06 ± 0.55*	0.45 ± 0.21
EMD					
$P_{R,LF}$	1.00 ± 0.35	0.90 ± 0.47	0.28 ± 1.60	0.96 ± 0.87	0.90 ± 0.78
$P_{R,HF}$	0.74 ± 0.31	0.83 ± 0.32	0.36 ± 1.40	0.18 ± 0.23*	1.30 ± 1.60
$\tilde{P}_{R,LF}$	0.60 ± 0.06	0.57 ± 0.05	0.43 ± 0.07*	0.75 ± 0.11*	0.40 ± 0.12*
$\tilde{P}_{R,HF}$	0.40 ± 0.06	0.43 ± 0.05	0.57 ± 0.07*	0.25 ± 0.11*	0.60 ± 0.12*
LF/HF	1.48 ± 0.30	1.35 ± 0.22	0.75 ± 0.23*	3.10 ± 2.40*	0.67 ± 0.36*

Standard vs. EMD-based spectral analysis indices for RR intervals. Low-frequency (LF) and high-frequency (HF), absolute (P) and normalized powers ($\tilde{P}$), and LF/HF ratio.
Top part: computed from standard spectral analysis (cf. section *Standard Spectral Analysis and Baroreflex Sensitivity*); bottom part: computed from EMD (cf. section *EMD and Baroreflex Sensitivity*). Powers are expressed in 10^3 ms^2/Hz. Results are expressed as in *Table I*.

Table III Standard vs. EMD-based spectral analysis indices for systolic blood pressure.

	Control	Saline (0.9%)	Phentolamine (10 mg/mL)	Atropine (10 mg/mL)	Atenolol (10 mg/mL)
Standard					
$P_{R,LF}$	0.29 ± 0.16	0.32 ± 0.16	0.28 ± 0.31	0.15 ± 0.13*	0.43 ± 0.43
$P_{R,HF}$	0.16 ± 0.08	0.18 ± 0.10	0.33 ± 0.17	0.10 ± 0.10*	0.92 ± 1.10
$\tilde{P}_{R,LF}$	0.64 ± 0.06	0.70 ± 0.05	0.51 ± 0.16	0.52 ± 0.10*	0.31 ± 0.10
$\tilde{P}_{R,HF}$	0.36 ± 0.06	0.30 ± 0.05	0.49 ± 0.16	0.48 ± 0.10*	0.69 ± 0.10
EMD					
$P_{R,LF}$	0.51 ± 0.30	0.52 ± 0.26	0.42 ± 0.42	1.80 ± 0.52*	0.35 ± 0.34
$P_{R,HF}$	0.14 ± 0.08	0.17 ± 0.09	0.24 ± 0.14	0.20 ± 0.05*	0.14 ± 0.14
$\tilde{P}_{R,LF}$	0.78 ± 0.06	0.79 ± 0.03	0.64 ± 0.16	0.89 ± 0.03*	0.77 ± 0.10
$\tilde{P}_{R,HF}$	0.22 ± 0.06	0.23 ± 0.03	0.37 ± 0.16	0.11 ± 0.03*	0.23 ± 0.10

Standard vs. EMD-based spectral analysis indices for systolic blood pressure. Low frequency (LF) and high frequency (HF), absolute (P) and normalized powers ($\tilde{P}$).
Top part: computed from standard spectral analysis (cf. section *Standard Spectral Analysis and Baroreflex Sensitivity*); bottom part: computed from EMD (cf. section *EMD and Baroreflex Sensitivity*). Powers are expressed in 10^3mmHg^2/Hz. Results are expressed as in *Table I*.

Table IV Standard versus EMD for Alpha Gains.

	Control	Saline (0.9%)	Phentolamine (10 mg/mL)	Atropine (10 mg/mL)	Atenolol (10 mg/mL)
Standard					
α_{LF}	0.07 ± 0.13	0.13 ± 0.13	0.07 ± 0.03	0.03 ± 0.01*	0.06 ± 0.05
α_{HF}	0.56 ± 0.49	0.59 ± 0.50	0.22 ± 0.22*	0.12 ± 0.02*	0.34 ± 1.00
EMD					
α'_{LF}	0.10 ± 0.12	0.14 ± 0.12	0.08 ± 0.08	0.03 ± 0.04*	0.05 ± 0.03*
α'_{HF}	0.68 ± 0.50	0.37 ± 0.40	0.16 ± 0.67	0.21 ± 0.06*	0.39 ± 1.20

Standard versus EMD alpha Gains in low frequency (α_{LF}) and high frequency (α_{HF}).
Top part: computed from standard spectral analysis (cf. section *Standard Spectral Analysis and Baroreflex Sensitivity*); bottom part: computed from EMD (cf. section *EMD and Baroreflex Sensitivity*). Results are expressed as in *Table I*.

this section aims at detailing practical issues in the implementation of the EMD procedure as well as the experimental results leading to the definition of the rules for the IMF association and hence to the EMD LF and HF decomposition.

Practical difficulties in implementation

Sampling rate

It has been observed empirically that the EMD procedure presents a better stability with respect to the frequency contents of the obtained IMFs when the analyzed data are sufficiently oversampled. It can be seen (cf. *Figures 1* and *2*) that the frequency contents of the data essentially vanish above 3 Hz. It has been chosen to sample the data at 10 Hz so that not only is the Shannon sampling theorem respected but data are also significantly oversampled. Higher oversampling frequencies do not improve the results but may induce significantly higher computational costs.

Sifting iteration number

As described in the section *EMD and Baroreflex Sensitivity* above, a key element in the construction of the IMF lies in the choice of a stopping criterion, qualifying how close it is from a zero-mean component and hence controlling the maximum number of allowed sifting iterations. Experimentally, we observed that allowing too many iterations is not desirable. It means first a high computational cost. Second and very importantly, it results in the creation of artificial frequency contents in IMFs. Indeed, to satisfy a severe stopping criterion, the EMD procedure tends to produce energy in the very low and low frequency ranges for the first IMF. Because EMD insures perfect reconstruction by linear addition of IMFs, this, in turns, also create artificial energy in the same frequency ranges for the subsequent IMFs, and hence a propagation of the defect across IMFs. A careful examination of the IMFs computed for each animal led us to choose to stop the sifting procedure either when a

non-severe criterion is satisfied or when a maximum number of iterations is reached. Practical experimentations led us to choose this maximum to 20. We carefully checked that the results reported in the present study do not depend on this precise choice of the iteration number and remain consistent when this number is varied from 15 to 100.

IMF frequency contents and EMD-based LF and HF decomposition

IMF frequency contents

Figures 3 and *4* present the superimposition of the spectra for IMF 1 to 6 obtained from all analyzed RR intervals and SBP time series, respectively. For RR intervals, *Figure 3* shows that the spectral contents of the four first IMFs fall within the HF and LF frequency bands, while all the subsequent IMFs are in the VLF frequency band or even below. This is why only the four first IMFs are considered for the RR interval time series. The same holds for the three first IMFs of the SBP time series. As an example, the periodogram based estimates of the spectra of the five first IMFs for RR intervals and SBP of two given rats are shown in *Figures 5* and *6*. For each IMF, the rigid position of the VLF, LF, HF bandwidth division are reported in black dashed vertical lines. The central frequency and the standard deviation spectral extension, that summarize the frequency content of the IMFs, are also represented with crosses. They are defined as in Eqn (8), mutatis mutandis.

Together, the examination of these four figures enable us to draw two major conclusions. First, in all cases IMFs with labels strictly larger than 4 correspond to VLF or even lower frequencies. They will not be further studied. Secondly, for RR interval time series, IMF1 and IMF2 have spectral contents that are systematically mainly spread within the HF band, while those of IMF3 and IMF4 fall in the LF band. For SBP time series, the spectrum of IMF1 corresponds to HF and those of IMF2 and IMF3 to LF. These considerations led us to propose the following EMD-driven definitions of the HF and LF contributions of the RR interval and SBP time series (cf. section *EMD and Baroreflex Sensitivity*):

$$\begin{aligned} R_{\mathrm{HF}}(t) &= \mathrm{IMF}_{\mathrm{R},1}(t) + \mathrm{IMF}_{\mathrm{R},2}(t), \\ R_{\mathrm{LF}}(t) &= \mathrm{IMF}_{\mathrm{R},3}(t) + \mathrm{IMF}_{\mathrm{R},4}(t), \\ P_{\mathrm{HF}}(t) &= \mathrm{IMF}_{\mathrm{P},1}(t), \\ P_{\mathrm{LF}}(t) &= \mathrm{IMF}_{\mathrm{P},2}(t) + \mathrm{IMF}_{\mathrm{P},3}(t). \end{aligned} \tag{9}$$

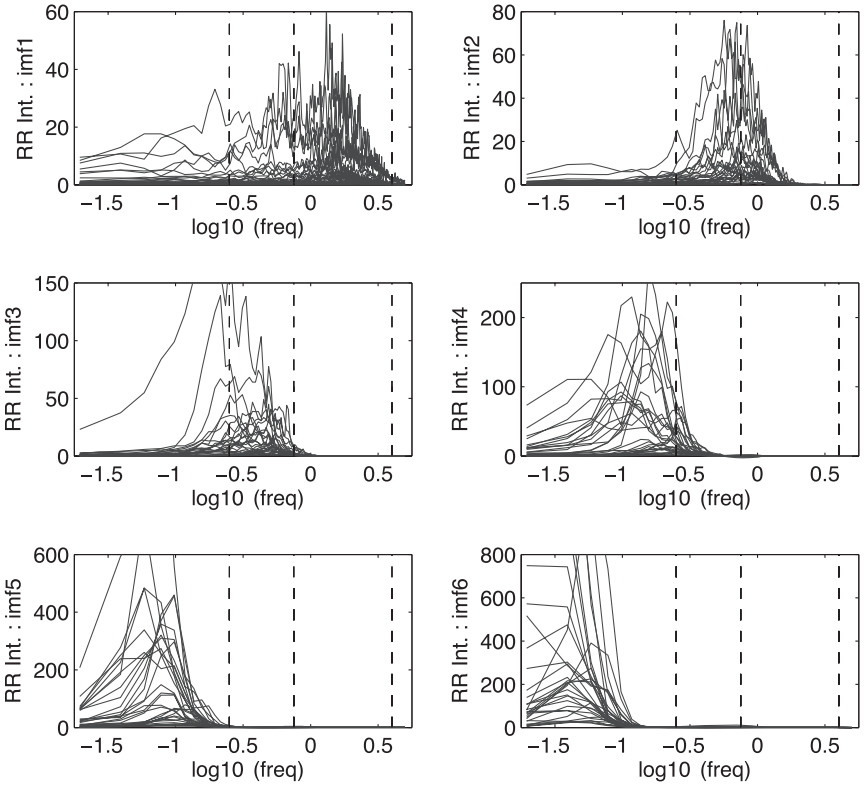

Figure 3 RR intervals IMFs for all animals. Superimposition of the 6 first IMFs for the RR Intervals signals of the 40 experiments (non-normalized log-lin plots). The vertical dashed lines show the VLF, LF and HF rigid a priori frequency bands. This shows that IMF1 and IMF2 are mainly concentrated in the HF band while that IMF3 and IMF4 essentially correspond to the LF one. IMF5 and those of higher order are clearly concentrated in the lower frequency ranges. HF = high frequency; IMF = intrinsic mode function; LF = low frequency; VLF = very low frequency.

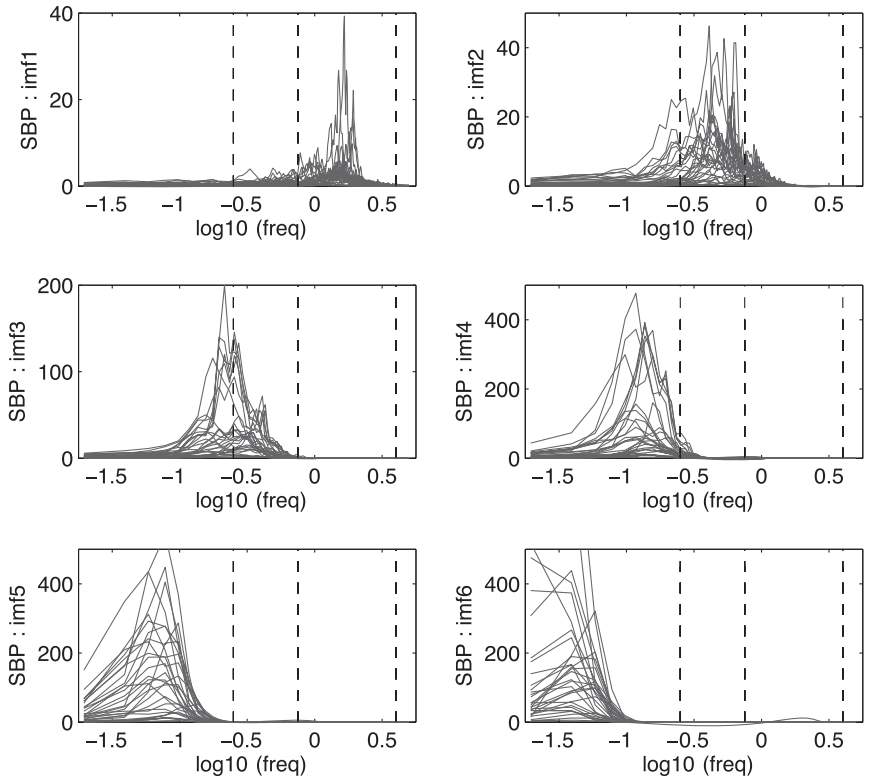

Figure 4 Systolic blood pressure IMFs for all animals. Superimposition of the 6 first IMFs for the systolic blood pressure (SBP) signals of the 40 experiments (non normalized log-lin plots). This shows that IMF1 is mainly concentrated in the HF band while that IMF2 and IMF3 essentially correspond to the LF one. IMF4 and of higher order are clearly concentrated in lower frequency ranges. IMF = intrinsic mode function; LF = low frequency.

We checked manually rat by rat and injection by injection that these associations are meaningful for each case.

EMD-based LF and HF decomposition

Figures 7 and *8* give examples of the spectral contents of R_{HF}, R_{LF}, P_{HF} and P_{LF} for two different animals, chosen as representative for the two characteristic situations practically observed: the EMD LF/HF decomposition matches the a priori rigid bands (example 1) or it does not (example 2). On the plots, the a priori LF/HF separations are shown with black dashed vertical lines, while the central frequency and the standard deviation spectral extension are pictured in solid line crosses. Their definitions are adapted straightforwardly from Eqn (8). *Figure 7* is representative for a large number of rats and injections, one sees that the frequency ranges of the EMD LF and HF contributions (R_{LF}, R_{LF} and P_{HF}, P_{HF}, respectively) spontaneously match those of the a priori rigid LF and HF bands. This is not an input of the approach and hence constitute per se a first interesting result validating the use of EMD: when the frequency contents of the data naturally match the a priori rigid LF and HF bands, EMD provides us with this decomposition.

Figure 8 shows the spectral contents of the LF and HF EMD components for another animal. For this particular individual, it can be noticed that, for both RR intervals and SBP, the LF components are significantly shifted towards lower frequencies. A large portion of the corresponding energy would have been considered VLF with the classical approach and not taken into account in the study of the sympathovagal balance while it is actually included in this balance determination with the EMD approach. This second example is chosen as a representative of a second group of (numerous) individuals, for which the EMD-based LF and HF components do not exactly match the rigid a priori frequency band decomposition.

In the former example, standard and non-standard spectral analyses yield equivalent values for the computed indices, while in the latter, significant differences are observed. Our interpretation of these discrepancies is as follows: The spectral content of the data that can be associated with the sympathetic and parasympathetic activities do not naturally fall exactly within the a priori chosen rigid frequency bands. Because of inter- and intra-individual natural or external variabilities, this bands may be slightly shifted from one measurement to the other and EMD spontaneously accounts for these natural variations [20,21]. The key point of our

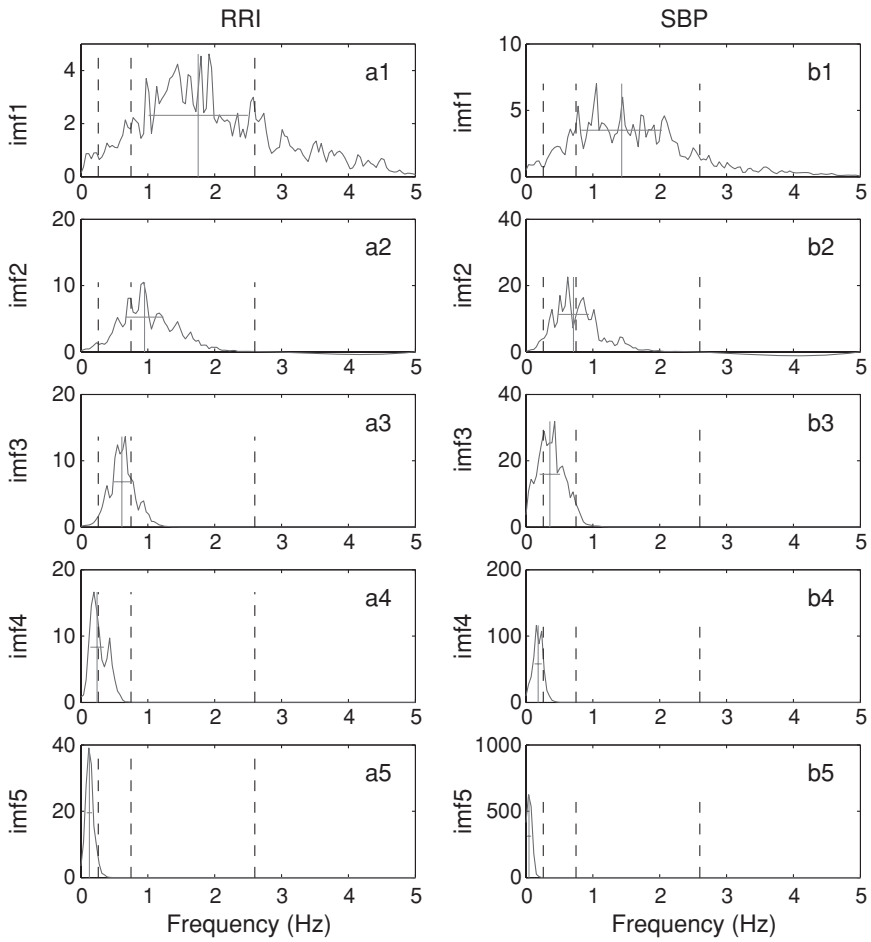

Figure 5 IMFs for Example 1. Spectral estimates for the five first IMFs for the RR Intervals (left column) and systolic blood pressure (right column) for the rat chosen as Example 1 in Figure 1. Vertical dashed lines indicate the VLF, LF and HF rigid a priori frequency bands. The solid line crosses denote the central frequency plus and minus one standard bandwidth (cf. Section 3.3.2 for definition) for each IMF. These plots highlight an example in which, for RR Intervals, the spectral contents of IMF1 and IMF2 are mainly spread in the HF band while the spectral contents of IMF3 and IMF4 essentially live in the LF one and in which, for systolic blood pressure, the spectral content of IMF1 is mainly spread in the HF band while the spectral contents of IMF2 and IMF3 essentially live in the LF one. Equivalent plots for each rat and each injection are available upon request. HF = high frequency; IMF = intrinsic mode function; LF = low frequency; VLF = very low frequency.

approach therefore lies in the fact that we obtain an LF vs. HF separation without resorting to a priori chosen and rigid band-pass filters. The a priori LF/HF separation defined above is now used only as a guideline to decide whether IMFs belong to LF or HF. This is the improvement brought about by the use of EMD.

EMD alpha gains: choosing the β parameter

The parameter β in Eqn (7) is related to the extension in the frequency domain of the spectra of the band-pass processes P_{LF} and P_{HF}. The choice of its value results from a trade-off that can be formulated as follows: a very large β would yield an overlap in the integration frequency bands and is hence against the intuition of a LF vs. HF decomposition. A very small β would result in highly fluctuating non-robust EMD alpha gains. Again, a careful examination of this issue led us to choose $\beta = 1$ (as represented in the figures). We checked that the results reported here do not significantly depend on the precise choice of β in a range $0.5 \leq \beta \leq 1.2$. Moreover, the ranges $\bar{f}_{P,LF} - \Delta f_{P,LF} \leq f \leq \bar{f}_{P,LF} + \Delta f_{p,LF}$ and $\bar{f}_{p,HF} - \Delta f_{p,HF} \leq f \leq \bar{f}_{p,HF} + \Delta f_{p,HF}$ tend to spontaneously match the a priori chosen widths of the LF and HF bands. This is not an a priori input of the method and can be considered as a significant a posteriori validation of the choice $\beta = 1$.

EXPERIMENTAL RESULTS

Time-domain analysis

Injections did not induce stress in animals and no signs of restlessness or irritation were noticed. After phentolamine administration, phenylephrine did not change systolic blood pressure ($\Delta = 5 \pm 3$ mmHg). Metacholine did not change RR intervals ($\Delta = 10 \pm 7$ ms) or SBP ($\Delta = -6 \pm 3$ mmHg) after atropine administration. Isoproterenol induced no significant change in RR intervals after atenolol administration ($\Delta = 10 \pm 8$ ms).

Time-domain measures of RR intervals and systolic and diastolic blood pressure are reported in *Table I*. Saline

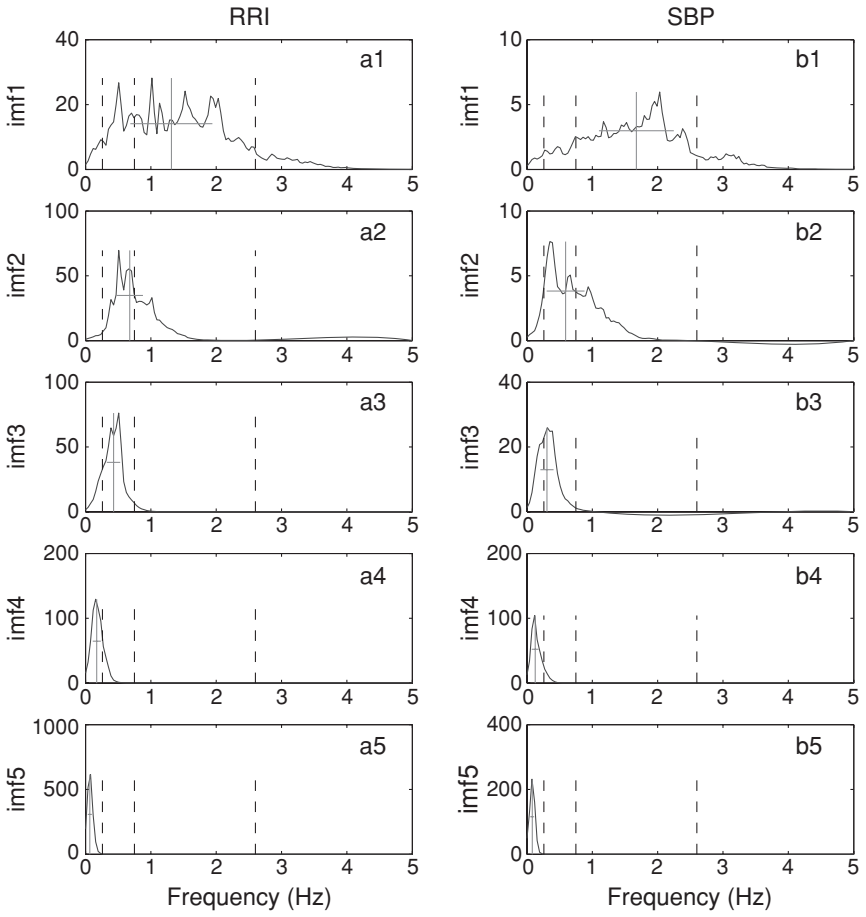

Figure 6 IMFs for Example 2. Spectral estimates for the five first IMFs for the RR Intervals (left column) and systolic blood pressure (right column) for the rat chosen as Example 1 in Figure 1. Vertical dashed lines indicate the VLF, LF and HF rigid a priori frequency bands. The solid line crosses denote the central frequency plus and minus one standard bandwidth (cf. Section 3.3.2 for definition) for each IMF. These plots highlight an example in which, for RR Intervals, the spectral contents of IMF1 and IMF2 are mainly spread in the HF band while the spectral contents of IMF3 and IMF4 essentially live in the LF one and in which, for systolic blood pressure, the spectral content of IMF1 is mainly spread in the HF band while the spectral contents of IMF2 and IMF3 essentially live in the LF one. Equivalent plots for each rat and each injection are available upon request. Compared with those in Figure 5, these plots show that the central frequencies are mostly shifted towards low frequencies.

injections do not induce any significant change in the global time-domain indices. All other injections do. Phentolamine reduced RR intervals by 30%, and systolic and diastolic blood pressure by 26% and 17%, respectively. Atropine reduced RR intervals by 24%, and increased systolic and diastolic blood pressure by 11% and 16%, respectively. Atenolol increased RR intervals by 11% and reduced systolic and diastolic blood pressure by 9%.

Standard spectral analysis

Tables II and *III* (top parts) summarize the values of various indices computed on RR intervals and SBP, respectively, using the standard spectral analysis and change detection test described above.

For RR intervals, atropine reduces LF (58%), HF (84%), normalized HF (19%) and increases LF/HF ratio (56%) and normalized LF (28%). For SBP, atropine induces a significant increase in LF (234%), HF (94%) and normalized LF (118%), and reduces normalized HF (34%). *Table IV* (top part) reports the changes in the alpha gains. Baroreflex sensitivity, measured by the LF and HF alpha gain indices, decreases after atropine (62% and 79%, respectively).

EMD-based spectral analysis

Tables II–IV (bottom parts) gather the values taken by the EMD-based spectral indices for RR intervals and SBP as well as alpha gains. For RR intervals, phentolamine increases the normalized HF (42%) while reducing normalized LF (28%) and LF/HF (49%). Atropine reduced HF (76%) and normalized HF (39%), and increased normalized LF (26%) and LF/HF (107%). Atenolol induced significant increase in normalized HF (48%) and reduced normalized LF (33%) and LF/HF (55%). For SBP, atropine reduces the normalized HF (52%) and increases the LF (253%), HF (50%) and normalized LF (15%). For baroreflex sensitivity, α'_{LF} is decreased after atropine and atenolol administration (72% and 50%, respectively) while α'_{HF} is decreased after atropine administration (69%).

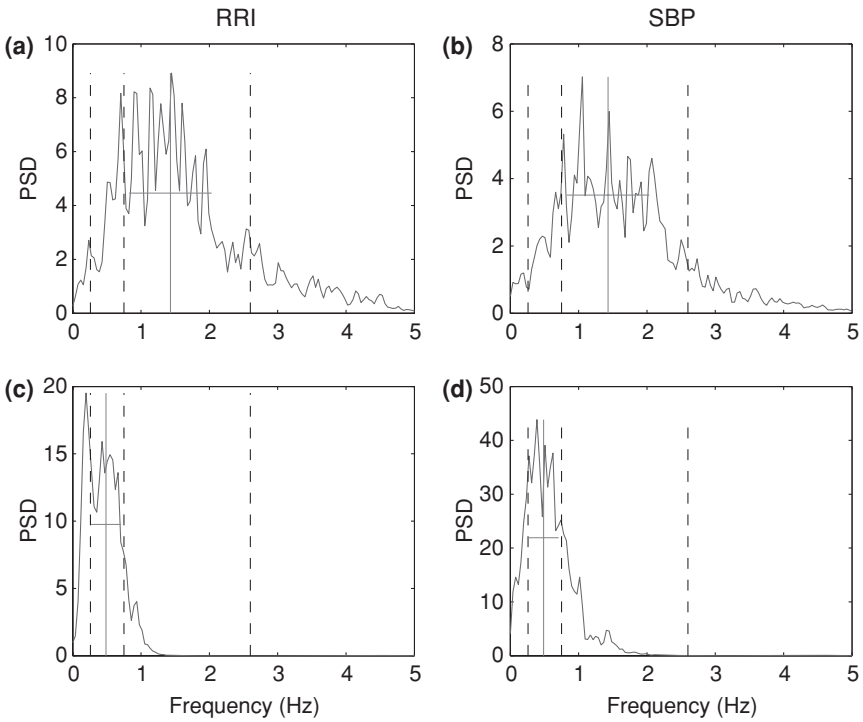

Figure 7 EMD-based LF and HF associations for Example 1. Spectral estimates for the HF (top) and LF (bottom) EMD based contributions for the RR Intervals (left column) and systolic blood pressure (right column) for the rat chosen as Example 1 in Figure 1. Vertical dashed lines indicate the VLF, LF and HF rigid a priori frequency bands. The solid line crosses denote the central frequencies plus and minus one standard bandwidth (computed from the SBP signal, cf. Section 3 for definition). These crosses delimitate the frequency bands over which the Alpha Gains are computed. In this example, one sees that the EMD-based HF and LF decomposition spontaneously matches the HF/LF a priori and rigid frequency band one. EMD = empirical mode decomposition; HF = high frequency; IMF = intrinsic mode function; LF = low frequency; VLF = very low frequency.

DISCUSSION

The combined use of a priori chosen and rigid frequency bands (and of the corresponding band pass filters) together with standard (parametric or non-parametric) spectral techniques, leading to the definitions of alpha gains as in Eqn (4), suffers from two major limitations [16]: First, they rely on a perfect stationarity assumption for the analyzed data. Secondly, they assume that the frequency band definitions used above in the LF vs. HF decompositions are absolute and cannot depend on the data. The EMD-based spectral analysis approach provides the user with a valuable tool to overcome those two difficulties [12,16,17].

In the present study, we mostly analyze animals under stable conditions so that the data remain stationary within the analysis time window. To that end, data are not collected immediately after injections, delay is respected to avoid transient behaviors. However, potential developments under investigations consist in studying transient states such as those observed during or just after injections. For such situations, producing highly non-stationary time series, we proposed, in a recent study, to define an extension of these gains that allowed us to study the evolution along time of the barosensitivity and derived the corresponding algorithm [15]. However, EMD also proves helpful. This is under investigation. For the work reported in the present contribution, the barosensitivity of the rats presents a strong and significant inter-animal variability. For instance, the frequency band decomposition corresponding to the sympathovagal balance may indeed slightly vary from one rat to the other according to its age, gender, etc. Moreover, it is well known that the barosensitivity of a given animal is likely to be spontaneously and dynamically modified or (slightly) shifted under an imposed change or external circumstances (such as stress, fatigue, respiration rate). To account for and accommodate both these inter and intra individual variations, we chose to use the EMD, because of its being a highly signal-adaptive frequency decomposition.

Let us now compare the results obtained from standard and EMD based spectral indices. For RR intervals, most of the significant changes detected by standard spectral analysis are also seen by EMD. For SBP, standard spectral analysis and EMD are in perfect agreement. These results can be read as a clear validation of the fact that the EMD-based spectral analysis proposed in the present study provides us with a meaningful spectral analysis tool.

One can further notice that for RR Intervals a number of significant changes are detected by EMD when they are missed by standard spectral analysis (cf. *Table II*). Let us carefully analyze these cases. A close inspection

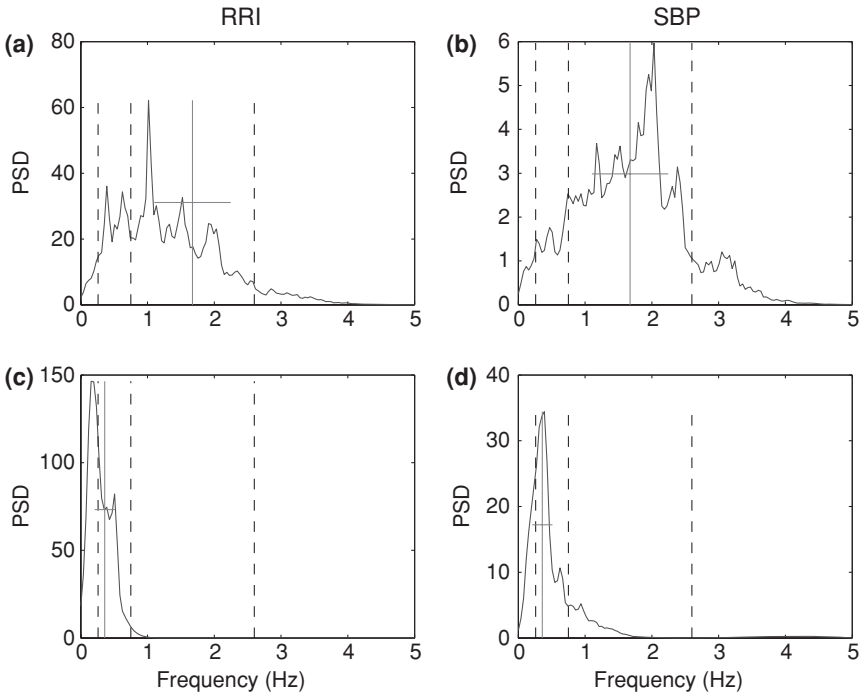

Figure 8 EMD-based LF and HF associations for Example 2. Spectral estimates for the HF (top) and LF (bottom) EMD based contributions for the RR Intervals (left column) and systolic blood pressure (right column) for the rat chosen as Example 1 in Figure 1. Vertical dashed lines indicate the VLF, LF and HF rigid a priori frequency bands. The solid line crosses denote the central frequencies plus and minus one standard bandwidth (computed from the SBP signal, cf. Section 3 for definition). These crosses delimitate the frequency bands over which the Alpha Gains are computed. Compared with those in Figure 7, these plots indicate that the EMD-based HF and LF separation may differ from the HF/LF a priori and rigid frequency band decomposition; here it is shifted towards low frequencies. This is where the EMD based non standard spectral analysis brings a significant contribution: it is signal adaptive so that it can spontaneously adjust to the natural shifts in the actual HF and LF frequency contents of the data. EMD = empirical mode decomposition; HF = high frequency; IMF = intrinsic mode function; LF = low frequency; VLF = very low frequency.

shows that for atenolol, detections are missed by standard spectral analysis because the *P*-values (not reported here for sake of clarity of the tables, but available upon request) are slightly above but very close to the 5% threshold value that yields a detection. Hence, we can argue that the EMD approach better takes into account the inter-individual variability and hence better achieves the LF and HF decomposition and the corresponding sympatovagal analysis. Therefore, it enables us to clearly detect changes that are significant and are only slightly missed by standard spectral analysis because of its rigid a priori choices.

For phentolamine, the situation is very different. Changes detected by EMD are totally missed by standard spectral analysis (the corresponding p-values are large). The reduction of the RR intervals normalized LF component after phentolamine administration, an α1-adrenoreceptor blocker, suggests a strong link between the RR intervals LF oscillations and the sympathetic vasomotor activity [5,6,22]. Moreover, it has been reported that phentolamine administration withdraws the vasomotor tone which is mainly sympathetic in rats [23,24].

Moreover, it is interesting to note that an increase in the RR interval-normalized HF component is observed after phentolamine injection (cf. *Table II*). In addition to its well-known ability to block α1-adrenoreceptors on vascular smooth muscles, phentolamine also has a central sympathetic withdrawal action, hence yielding an RR interval-normalized HF increase [24,25].

Therefore, in comparison with standard spectral analysis that misses sympathovagal balance alterations after phentolamine administration, EMD hence shows a better ability to detect them. Let us now turn to baroreflex sensitivity. LF baroreflex sensitivity decreases after atropine and atenolol. However, it is reduced less by beta-blockade than it is by administration of atropine, indicating the predominance of vagal effects in this measure of the baroreflex sensitivity [21]. Therefore, it is

worth noting here that the EMD-based LF alpha gain index detects changes both for atropine and atenolol while the standard spectral analysis one is blind to the latter (cf. *Table IV*).

For HF baroreflex sensitivity, both tools detect the change induced by atropine. For phentolamine, the standard index sees a change when the EMD-based one does not (cf. *Table IV*). This may be explained by the effect of respiration on RR intervals, known as the respiratory sinus arrhythmia. Without standardization against the respiratory rate (which we did not measure in our study), HF changes cannot be fully and relevantly studied [26,27]. Therefore, in all situations where discrepancies between the results obtained with EMD and standard spectral analysis were observed, a number of arguments can be proposed that indicate that EMD provides us with a finer analysis of the sympathovagal balance modifications.

CONCLUSION AND PERSPECTIVES

In the present study, we assessed the relevance of various spectral indices for the detection and analysis of changes in the sympathovagal balance. We showed that the use of a non-standard spectral analysis based on EMD brings improvements compared with standard spectral analysis. This is mainly because it is able to account for the natural intra- and inter-individual variabilities. Indeed, it avoids the drawbacks induced by the choice of a priori, rigid, and uniform, for all individuals, band-pass filters. Furthermore, we showed that the use of EMD requires significant attention regarding implementation issues such as sampling rate, sifting procedure, stopping criterion, IMF association procedure and alpha gain definitions. The EMD-based spectral analysis requires further developments under investigations to be made fully automatic. The next step of the validation of the EMD improvements is to apply it to the standard data for comparison of the spontaneous baroreflex (the EuroBaVar study).

Because EMD is naturally designed to address non-stationarities, the non-standard spectral analysis developed here could be fruitfully extended to situations where a dynamical change is imposed to the study the dynamical behaviour of the baroreflex sensitivity. This EMD approach can also relevantly be compared with other approaches based on time–frequency representations that provide indications regarding the way the spectral energy distribution of a signal varies along time [20,28,29]. Moreover, we believe that the potentialities of the EMD-based approach developed here are such that it could be successfully used in other physiological situations to provide new observations more directly applicable to research in physiology [30]. Further studies are necessary in animals and in humans to assess the use of this method to study alterations induced by hypertension, diabetes or other transition periods like arrhythmia.

ACKNOWLEDGEMENTS

This work was supported by grants from the Centre National d'Etudes Spatiales (CNES) and Groupement d'Intérêt Public (GIP) Exercice. The authors gratefully acknowledge Gabriel Rilling, PhD student at ENS Lyon, who helped them in adapting and in modifying the EMD routines. The authors gratefully acknowledge two anonymous reviewers for fruitful comments and careful reading that substantially helped in improving the original manuscript.

REFERENCES

1 Ori Z., Monir G., Weiss J., Sahyouni X.N., Singer, D.H. Heart rate variability: frequency domain analysis. Cardiol. Clin. (1992) **10** 499–538.
2 Goldberger J.J. Sympathovagal balance: how should we measure it? Am. J. Physiol. (1999) **45** H1273–H1280.
3 Parati G., Saul J.P., Di Rienzo M., Mancia G. Spectral analysis of blood pressure and heart rate variability in evaluating cardiovascular regulation – a critical appraisal. Hypertension (1995) **25** 1276–1286.
4 Stein P.K., Kleiger R.E. Insights from the study of heart rate variability. Annu. Rev. Med. (1999) **50** 249–261.
5 Pagani M., Lombardi F., Guzzetti S. et al. Power spectral analysis of heart rate and arterial pressure variabilities as a marker of sympathovagal interaction in man and conscious dog. Circ. Res. (1986) **59** 179–193.
6 Malliani A., Pagani M., Lombardi F., Cerutti S. Cardiovascular neural regulation explored in the frequency domain. Circulation (1991) **84** 482–492.
7 Eckberg D.L. Sympathovagal balance: a critical appraisal. Circulation (1997) **96** 3224–3232.
8 Pomeranz B., MaCaulay R.J.B., Caudill M.A. et al. Assessment of autonomic function in humans by heart rate spectral analysis. Am. J. Physiol. (1985) **248** H151–H153.
9 Farah V.M.A., Moreira E.D., Pires M.D., Irigoyen M.C.C. Krieger, E.M. Comparison of three methods for the determination of baroreflex sensitivity in conscious rats. Braz. J. Med. Biol. Res. (1999) **32** 361–369.
10 Laude D., Elghozi J.L., Girard A. et al. Comparison of various techniques used to estimate spontaneous baroreflex sensitivity (the EuroBaVar study). Am. J. Physiol. (2004) **286** R226–R23.

11 Souza Neto E.P., Custaud M.A, Cejka J.C. et al. Assessment of cardiovascular autonomic control by the empirical mode decomposition. Proceedings IV InternationalWorkshop Biosignal Interpretation BSI2002, Como, Italy, 2002, pp. 123–126.
12 Huang N.E., Shen Z., Long S.R. et al. The empirical mode decomposition and the Hilbert spectrum for nonlinear and non-stationary time series analysis. Proc. R. Soc. Lond. A. (1998) **454** 903–995.
13 Huang N.E., Shen S.S.P., eds. Hilbert-Huang transform and its applications. World Scientific, Singapore. 2005.
14 Souza Neto E.P., Custaud M.A, Frutoso J., Somody L., Gharib C., Fortrat J.O. Smoothed pseudo Wigner-Ville distribution as an alternative to Fourier transform in rats. Auton. Neurosci. (2001) **87** 258–267.
15 Custaud M.A., Souza Neto E.P., Abry P. et al. Orthostatic tolerance and spontaneous baroreflex sensitivity in men versus women after 7 days of head-down bed rest. Auton. Neurosci. (2002) **100** 66–76.
16 Huang W., Shen Z., Huang N.E., Fung Y.C. Use of intrinsic modes in biology: examples of indicial response of pulmonary blood pressure to +/− step hypoxia. Proc. Natl. Acad. Sci. U.S.A. (1998) **95** 12766–12771.
17 Huang W., Shen Z., Huang N.E., Fung Y.C. Nonlinear indicial response of complex nonstationary oscillations as pulmonary hypertension responding to step hypoxia. Proc. Natl. Acad. Sci. U.S.A. (1999) **96** 1834–1839.
18 Echeverria J.C., Crowe J.A., Woolfson M.S., Hayes-Gill B.R. Application of empirical mode decomposition to heart rate variability analysis. Med. Biol. Eng. Comput. (2001) **39** 471–479.
19 Auger F., Flandrin P., Gonçalvès P., Lemoine O. Time-frequency toolbox for Matlab. Available at http://perso.ens-lyon.fr/Patrick.flandrin.
20 Novak P., Novak V. Time/frequency mapping of the heart rate, blood pressure and respiratory signals. Med. Biol. Eng. Comput. (1993) **31** 103–110.
21 Ramaekers D., Beckers F., Demeulemeester H., Aubert A.E. Cardiovascular autonomic function in conscious rats: a novel approach to facilitate stationary conditions. Ann. Noninvasive Electrocardiol. (2002) **7** 307–318.
22 Rubini R., Porta A., Baselli G., Cerutti S., Paro M. Power spectrum analysis of cardiovascular variability monitored by telemetry in conscious unrestrained rats. J. Auton. Nerv. Syst. (1993) **45** 181–190.
23 Akselrod S., Eliash S., Oz O., Cohen S. Hemodynamic regulation in SHR: investigation by spectral analysis. Am. J. Physiol. (1987) **253** H176–H183.
24 Herijgers P., Flameng W. The effect of brain death on cardiovascular function in rats. Part II. The cause of the in vivo haemodynamic changes. Cardiovasc. Res. (1998) **38** 107–115.
25 Hilliard C.C., Bagwell E.E., Daniell H.B. Effects of sympathetic and central nervous system alterations on the blood pressure responses to phentolamine. J. Pharmacol. Exp. Ther. (1972) **180** 743–747.
26 Saul J.P., Berger R.D., Chen M.H., Cohen R.J. Transfer function analysis of autonomic regulation. II. Respiratory sinus arrhythmia. Am. J. Physiol. (1989) **256** H153–H161.
27 Perlini S., Giangregorio F., Coco M. et al. Autonomic and ventilatory components of heart rate and blood pressure variability in freely behaving rats. Am. J. Physiol. (1995) **269** H1729–H1734.
28 Cohen L. Time-frequency analysis. Prentice-Hall, Englewood Cliffs, NJ. 1995.
29 Flandrin P. Time-frequency/time-scale analysis. Academic Press, San Diego, 1999.
30 Gustin M.P., Cerutti C., Unterreiner R., Paultre C. Identification of spontaneous cardiac baroreflex episodes at different time-scales in rats. Am. J. Physiol. (1998) **274** H488–H493.